npj | precision oncology

Article

Published in partnership with The Hormel Institute, University of Minnesota

https://doi.org/10.1038/s41698-024-00645-3

Peptide-stimulated T cells bypass immune checkpoint inhibitor resistance and eliminate autologous microsatellite instable colorectal cancer cells

Sandra Schwarz[1], Zhaoran Su[1], Mathias Krohn[1], Markus W. Löffler[2,3,4,5,6], Andreas Schlosser[7] & Michael Linnebacher[1]

Two hypermutated colon cancer cases with patient-derived cell lines, peripheral and tumor-infiltrating T cells available were selected for detailed investigation of immunological response.
T cells co-cultured with autologous tumor cells showed only low levels of pro-inflammatory cytokines and failed at tumor recognition. Similarly, treatment of co-cultures with immune checkpoint inhibitors (ICI) did not boost antitumor immune responses. Since proteinase inhibitor 9 (PI-9) was detected in tumor cells, a specific inhibitor (PI-9i) was used in addition to ICI in T cell cytotoxicity testing. However, only pre-stimulation with tumor-specific peptides (cryptic and neoantigenic) significantly increased recognition and elimination of tumor cells by T cells independently of ICI or PI-9i.
We showed, that ICI resistant tumor cells can be targeted by tumor-primed T cells and also demonstrated the superiority of tumor-naïve peripheral blood T cells compared to highly exhausted tumor-infiltrating T cells. Future precision immunotherapeutic approaches should include multimodal strategies to successfully induce durable anti-tumor immune responses.

The interaction of tumor with immune cells triggers dynamic adaption to evade immunosurveillance. A prominent example is tumors' genetic or epigenetic modifications to reduce or switch-off HLA class I expression, thus preventing detection by T cells. Depending on the tumor entity, up to 80 % of solid tumors have completely lost HLA class I expression[1]. Another tool to repress antitumor immune responses is the expression of immunomodulatory proteins like programmed cell death protein 1 (PD-1), cytotoxic T lymphocyte associated protein 4 (CTLA-4) and lymphocyte activation gene 3 (LAG-3) or their respective ligands in the tumor microenvironment[2]. Via these immune checkpoint molecules, tumor cells utilize the physiologically programmed down-modulation of activated immune cells. However, therapeutic interfering with these immunosuppressive mechanisms via immune checkpoint inhibitors (ICI) represents the latest revolution in cancer treatment.

The application of ICI is mostly limited to tumors with high mutational burden (TMB), since clinical trials proved highest response rates in this patient group (reviewed in ref. 3). However, despite preselection of patients, studies with microsatellite instable colorectal cancer (CRC) revealed, that up to 70 % of patients do not benefit from pembrolizumab[4], nivolumab[5] or durvalumab[6] treatment. Although the combination of ipilimumab and nivolumab has been shown to increase the patients' objective response rate to 55 %[7], a substantial number of hyper-mutated tumors remains resistant to ICI treatment.

High TMB and constitutive HLA class I expression are both favorable prognostic markers for immunotherapy[8,9], but ICI therapy response prediction remains unsatisfactory. High TMB of ≥10 mutations/Mb is insufficient to predict ICI success, neither across cancer entities nor within a specific one[10,11]. However, the

[1]Department of General Surgery, Molecular Oncology and Immunotherapy, University Medicine Rostock, Rostock, Germany. [2]Department of General, Visceral and Transplant Surgery, University Hospital Tübingen, Tübingen, Germany. [3] Institute of Immunology, University of Tübingen, Tübingen, Germany. [4]German Cancer Consortium (DKTK) and German Cancer Research Center (DKFZ) Partner Site Tübingen, Tübingen, Germany. [5]Cluster of Excellence iFIT (EXC2180) 'Image-Guided and Functionally Instructed Tumor Therapies', University of Tübingen, Tübingen, Germany. [6]Institute for Clinical and Experimental Transfusion Medicine, Medical Faculty, University Hospital Tübingen, Tübingen, Germany. [7]Rudolf-Virchow Center, Center for Integrative and Translational Bioimaging, University of Würzburg, Würzburg, Germany.
e-mail: michael.linnebacher@med.uni-rostock.de

combination of TMB and loss of heterozygosity in HLA class I improved differentiation between ICI therapy responders and non-responders in lung cancer[12,13]. Similarly, a score retrospectively determining tumor immunogenicity by TMB combined with antigen processing machinery gene expression improved ICI therapy response prediction in urothelial cancer and melanoma datasets[14].

T cells interaction with tumors can further be impaired by several other immunosuppressive mechanisms beyond dysfunctional antigen presentation. Malignant cells often secrete immune regulatory molecules, e.g., cytokines, which exert immunosuppressive effects in the tumor microenvironment[15,16]. Likewise, enzymes and enzyme inhibitors with a role in regulating immune cell activity have been identified as complementary tumor immune evasion strategies[17,18].

Here, we selected two microsatellite instable CRC cases exhibiting constitutive HLA expression and investigated the interaction of T cells with autologous tumor cells ex vivo. Co-culture of tumor cells with autologous peripheral (pTc) or tumor-infiltrating T cells (TiTc) was applied to test the antitumor effect of isolated T cells alone or in combination with immune modulatory agents matching tumor cells' characteristics. Moreover, effects of individualized inhibition of immunosuppression were directly compared to anti-tumor immune responses of autologous T cells recognizing tumor-specific antigenic peptides.

Results

Selection of tumor cases

For a detailed analysis of tumor and T cell interactions, appropriate patient biomaterials were selected from our comprehensive set of CRC models available at the BioBank Rostock[19].

Considering all decisive factors (biomaterial availability, frequent non-synonymous mutations, antigen processing, HLA class I expression, and HLA class II inducibility), the two CRC cases HROC113 and HROC285 were selected. Both tumors showed high TMB (HROC113: 176 mutations/Mb; HROC285: 212 mutations/Mb) and microsatellite instability (MSI). Tumor cell lines were established directly from the patient's tumor (HROC113) or from a patient-derived xenograft (HROC285 T0 M2). Tumor-infiltrating T cells (TiTc) and peripheral T cells (pTc) as well as B-lymphoblastoid cell lines (B-LCLs) were also available for both patients.

T cells do not get activated by co-culture with autologous tumor cells

Co-culture experiments of T cells and autologous tumor cells were performed to investigate if the tumors with high TMB and HLA expression can induce sufficient immune responses. Tumor cells were incubated with T cells, which were pre-treated as follows: (1) expanded T cells, (2) T cells, which were expanded and subsequently co-cultured with autologous tumor cells for 14 days and (3) T cells, which were expanded and subsequently cultured for 14 days in the same conditions (temperature, media, supplements, change of media) but without tumor cells (=control culture with tumor-naïve T cells). In the degranulation assay (Fig. 1a, Supplementary Fig. 1), the amount of T cells recognizing tumor cells ($CD8^+/CD107a^+/IFN\gamma^+$ cells) was larger in co-cultured compared to unspecifically expanded pTc HROC113 ($p = 0.04$). Similarly, more degranulating T cells were detected among tumor-naïve pTc HROC113 from the control culture than among unspecifically expanded pTc HROC113 ($p = 0.02$). There was no significant difference observed between the reactivity of co-cultured and control-cultured pTc HROC113 ($p > 0.05$; Fig. 1a). The TiTc HROC113 showed a

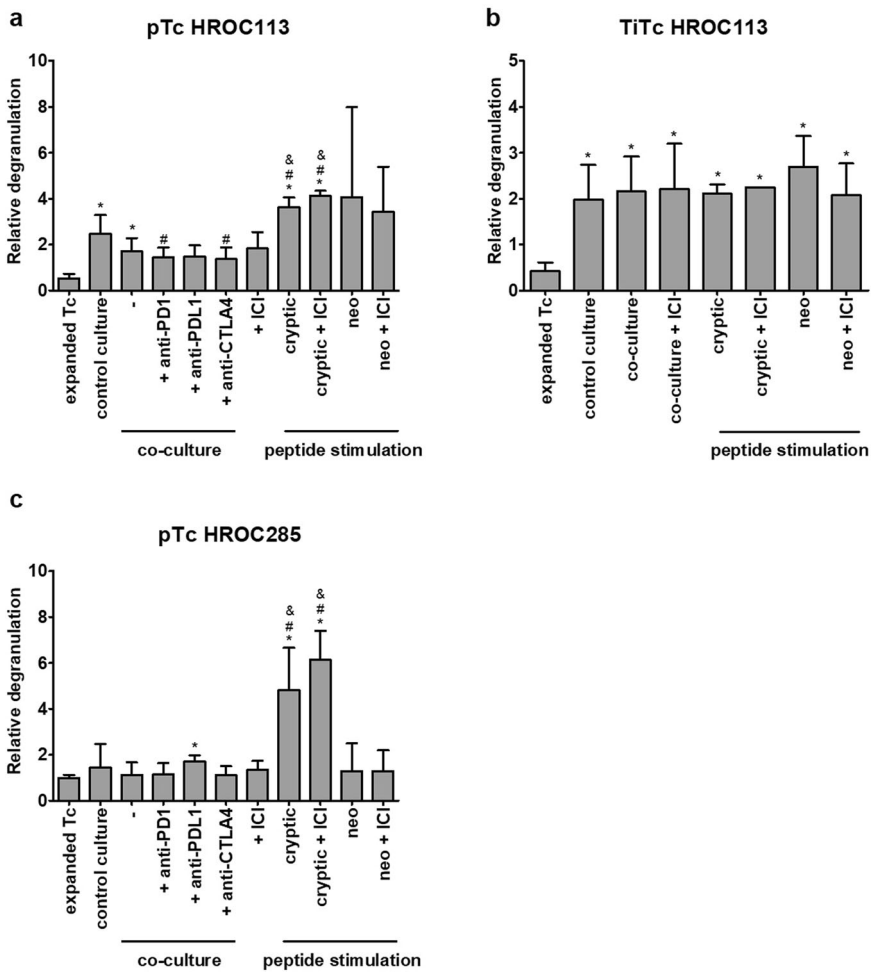

Fig. 1 | Effect of co-culture, ICI treatment and peptide stimulation on tumor cell recognition by Tc. a pTc HROC113, (**b**) TiTc HROC113 and (**c**) pTc HROC285 underwent different (co-)culture conditions or were stimulated with tumor-specific peptides to increase their antitumor reactivity measured by degranulation assay after 5 h incubation with freshly prepared tumor cells. $CD8^+/CD107a^+/IFN\gamma^+$ cells were considered tumor-reactive. Results were normalized to measurements of control Tc not incubated with tumor cells. $p < 0.05$ in *t*-test of sample vs. expanded T cell (*), control culture (#) or co-culture (&). Depicted are means of 2–6 biological replicates and the respective standard deviation.

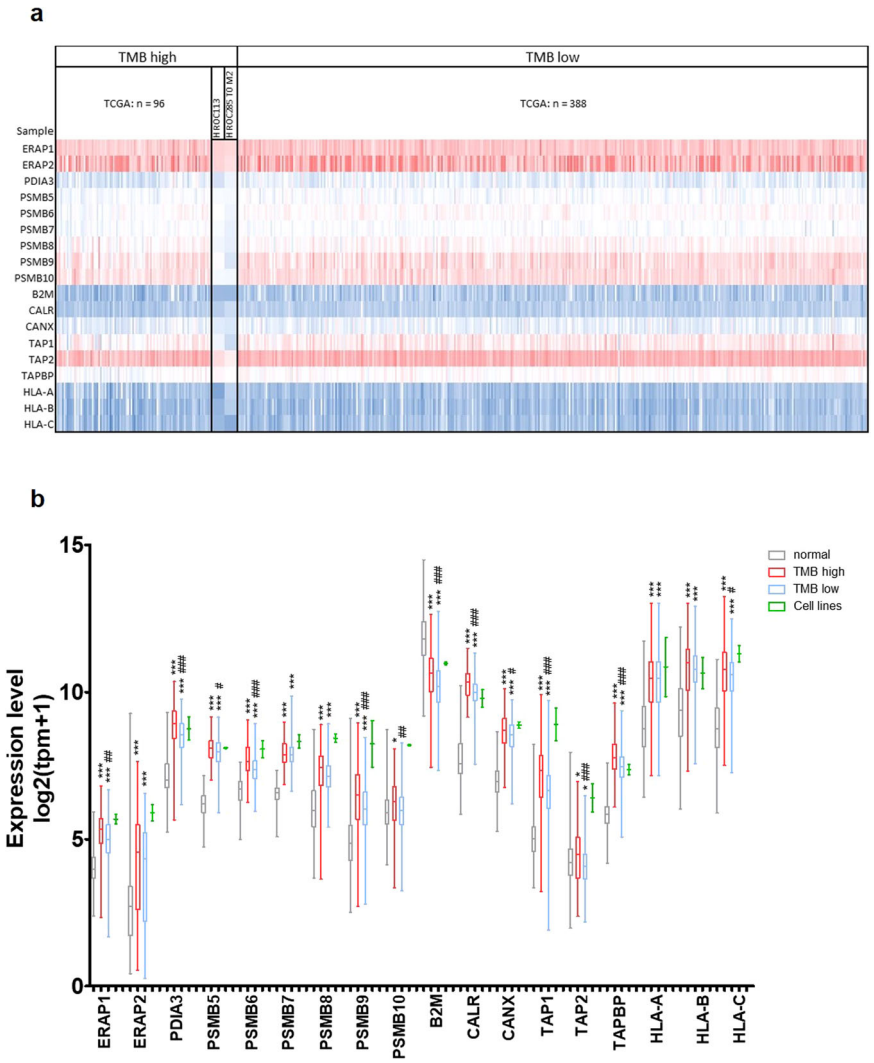

Fig. 2 | Expression of genes involved in antigen processing. TCGA data of CRC ($n = 484$) were compared with normal colon tissue (TCGA: $n = 51$, GTEX: $n = 308$) and tumor cell lines ($n = 2$), regarding expression of 18 genes involved in antigen processing and presentation. Tumor cell line data contained three technical replicates each, but due to the small group size, statistical calculations were omitted. **a** Heatmap of analyzed data sets depicting high expression in blue and low expression in red, in regard to TMB. **b** Mean expression of antigen processing genes including standard deviation; *t* test of tumor sample vs. normal tissue with $p < 0.05$ (*), $p < 0.01$ (**) and $p < 0.001$ (***); *t* test of TMB high vs. TMB low with $p < 0.05$ (#), $p < 0.01$ (##) and $p < 0.001$ (###).

similar pattern (Fig. 1b) and corroborated the previous results ($p_{\text{co-culture vs expanded Tc}} = 0.02$; $p_{\text{control-culture vs expanded Tc}} = 0.03$; $p_{\text{co-culture vs control culture}} > 0.05$). In contrast, the population of tumor-reactive cells among pTc HROC285 was similar in all three tested conditions (unspecific expansion, co-culture, control culture) and no distinct differences were observed (Fig. 1c). TiTc HROC285 were also assessed using this experimental approach but unfortunately the proportion of $CD8^+$ cells, being as low as 27 % in the beginning, even decreased further during the cultivation period and no reliable measurements of $CD8^+/CD107a^+/IFN\gamma^+$ cells could be obtained.

ICI do not increase the recognition of autologous tumor cells by T cells

Since tumor cells failed to induce T cell responses, ICI (pembrolizumab (anti-PD-1), durvalumab (anti-PD-L1), and ipilimumab (anti-CTLA-4)) were added to the co-culture to improve anti-tumor reactions. Contrasting expectations, pTc HROC113 recognized tumor cells better after control culture than after ICI-supplemented co-culture, showing significantly deterioration after co-culture with PD-1 or CTLA-4 supplementation ($p = 0.048$ and $p = 0.041$, respectively) (Fig. 1a). Moreover, the degranulation capacity of co-cultured pTc HROC113, with and without ICI treatment, was significantly lower compared to tumor-naïve pTc HROC113 ($p = 0.004$).

Due to the low quantity of available TiTc HROC113, single ICI testing was replaced by a combination treatment (Fig. 1b) but did also not improve tumor cell recognition. The results of pTc HROC285 (Fig. 1c) resembled those of pTc HROC113: tumor-naïve pTc HROC285 showed high degranulation, contrasting co-cultured pTc HROC285 with decreased tumor cell recognition. The addition of ICI was insufficient to overcome the tumor cell-induced T cell inhibition.

HROC113 and HROC285 T0 M2 express genes of the antigen-processing machinery

To investigate reasons for the failure of ICI treatment in vitro, we analyzed the expression of genes involved in antigen processing and presentation. By determining the expression of 18 genes used in the study of ref. 14, their immunological functionality was assessed in the established tumor cell lines. Respective results were compared to datasets of normal colon and CRC samples from TCGA and GTEX (Colon: TCGA normal: $n = 51$; TCGA tumor: $n = 484$; GTEX normal: $n = 308$). Surprisingly, when compared to normal colon samples, gene expression was higher in both tumor cell lines as well as in TMB high and TMB low tumor tissues regarding 16/18 genes investigated (Fig. 2a, b). Only the expression of β2 microglobulin (B2M) was found significantly lower in tumor tissues compared to healthy colon samples in the analyzed data sets. When assessing differing genes between TMB high and low CRC tissue samples, we observed, that the expression level of ERAP1, PDIA3, PSMB6, PSMB9, PSMB10, CALR, CANX, TAP1, TAP2, TAPBP, B2M, and HLA-C was found to be lower in tumors featuring fewer mutations. In both tumor cell lines, the mean expression of the selected genes resembled or even

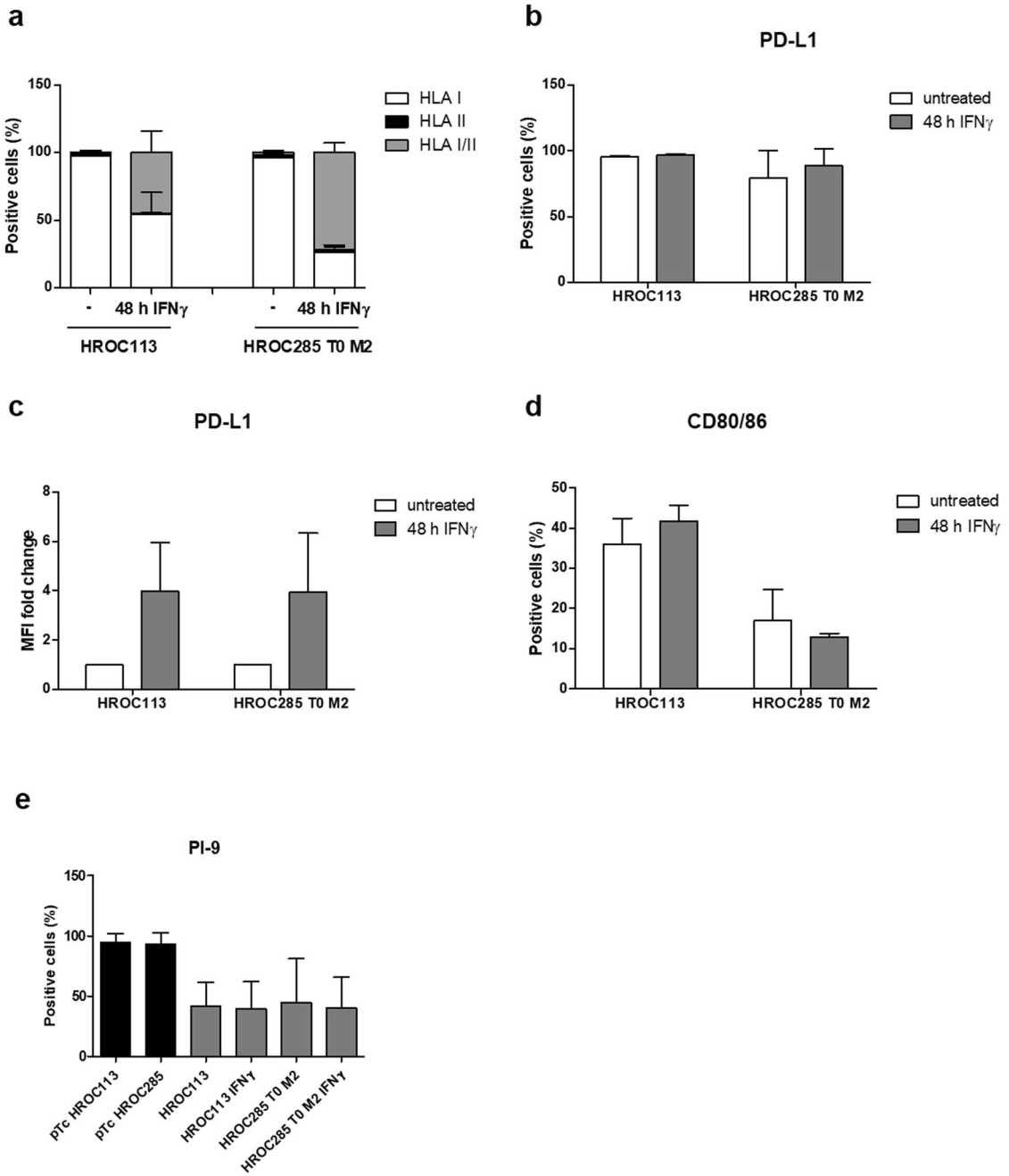

Fig. 3 | Tumor cell characterization. Untreated or IFNγ-treated (200 IU/ml for 48 h) tumor cells were analyzed via flow cytometry. Percentage of HLA class I- and II-positive cells were measured (**a**). PD-L1-positive tumor cells were detected and percentages (**b**) and median fluorescence intensity (**c**) are depicted. Percentages of CD80/86- (**d**) and PI-9-positive cells (**e**) were determined. Depicted are means of 3–5 biological replicates and the respective standard deviation.

exceeded the levels in CRC samples from TCGA, but due to the small size of the cell line cohort ($n = 2$), statistical analysis was inadmissible. Moreover, functional antigen processing was previously assured through HLA ligandome analyses enabling the characterization of several thousand HLA ligands for each CRC cell line, including tumor-specific antigens[20].

Flow-cytometry analyses showed that 98 % of HROC113 and 96 % of HROC285 T0 M2 cells stained positive for HLA class I (Fig. 3a). IFNγ pre-treatment increased the amount of HLA class I/II double positive cells in HROC113 from < 1 % to 45 % ($p < 0.001$). In HROC285 T0 M2, the proportion of HLA class I^+/II^+ cells even reached 72 % following IFNγ treatment compared to 2 % in untreated cells ($p < 0.001$). Accordingly, median fluorescence intensity of HLA class II increased by 20-fold after IFNγ stimulation ($p = 0.002$). Thus, IFNγ pre-treatment was performed for all the following experiments.

These results prove the integrity of antigen presentation in the selected tumor cell lines suggesting functional immune interaction with autologous lymphocytes. Thus, the observed immunosuppression by the tumor cells must be ascribed to other immune evasion mechanisms.

Tumor cells utilize several immunosuppressive mechanisms

Expression of the inhibitory checkpoint molecule programmed death-ligand 1 (PD-L1) was observed in the majority of tumor cells (HROC113: 95 %; HROC285 T0 M2: 79 %; Fig. 3b, c, Supplementary Fig. 2). Here, stimulation with IFNγ increased median fluorescence intensity of PD-L1

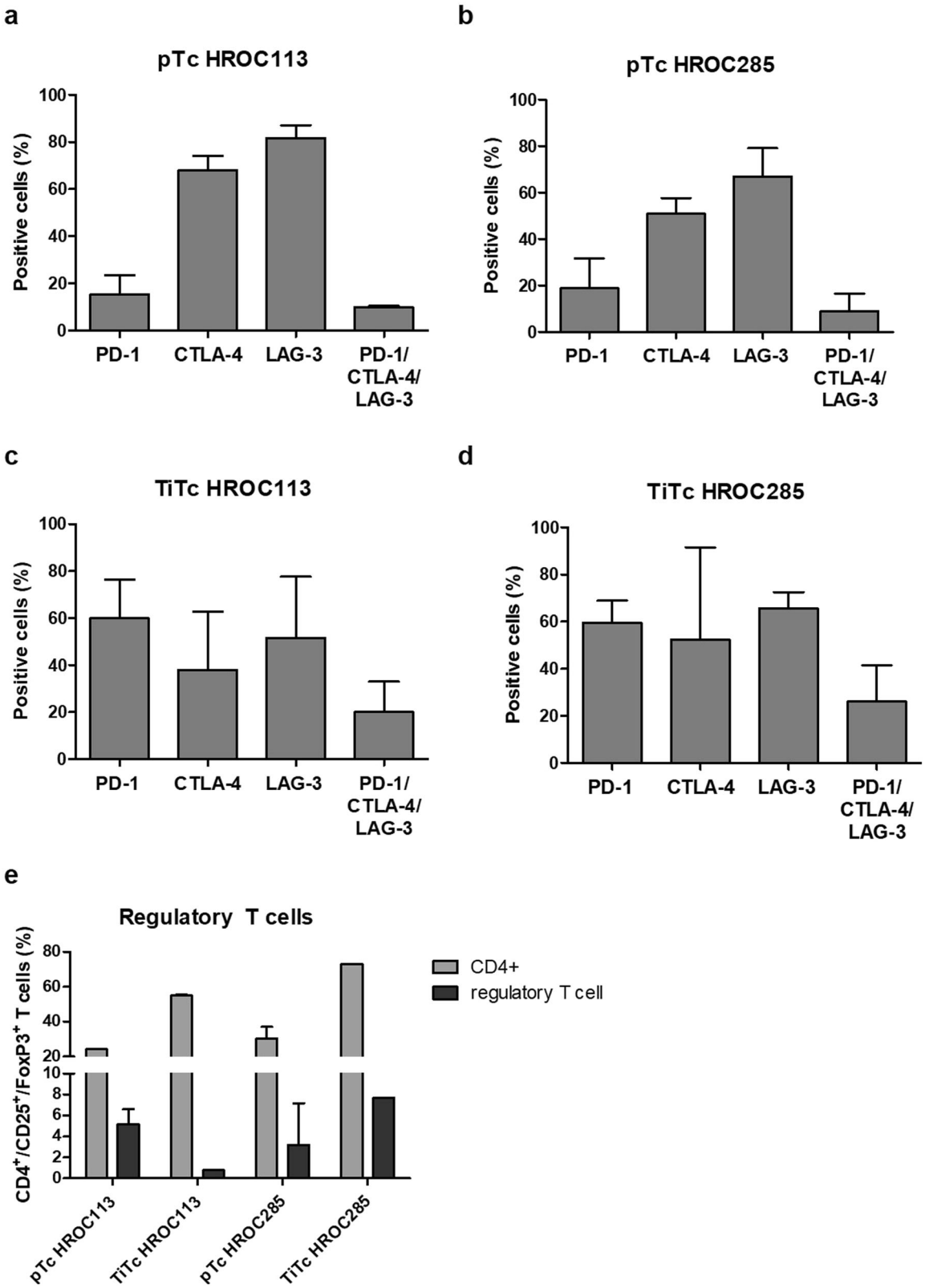

Fig. 4 | Characterization of T cells. Following 14 days of unspecific expansion, Tc were analyzed regarding (**a**–**d**) exhaustion markers and (**e**) proportion of regulatory Tc defined as $CD4^+/CD25^+/FoxP3^+$. Depicted are means of 3–4 biological replicates and the respective standard deviation.

expression about 4-fold in both tumor cell lines ($p = 0.05$ in both cases). When determining CD80/86 expression, this CTLA-4 ligand was detected on 30 % and 17 % of HROC113 and HROC285 T0 M2 cells, respectively (Fig. 3d). Treatment with IFNγ did not significantly change CD80/86 expression.

Further characterization of the tumor cells revealed granzyme B activity in HROC113 as well as HROC285 T0 M2, which was found independent of IFNγ treatment (Supplementary Fig. 3). As this apoptosis-propagating enzyme threatens cell survival, its presence is often accompanied by the expression of proteinase inhibitor 9 (PI-9), which specifically

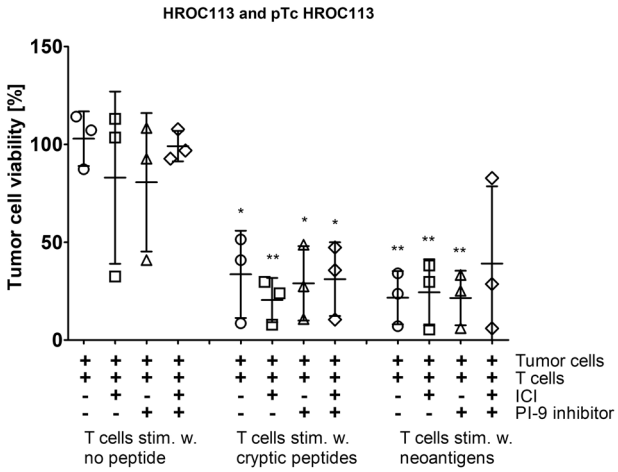

Fig. 5 | Cytotoxicity of pTc HROC113. Tumor cells were incubated for 48 h with pTc HROC113, which were pre-stimulated for 14 days with tumor-specific cryptic or neoantigenic peptides. pTc HROC113 stimulated without peptide served as control. Medium was supplemented with three ICI (20 µg/ml pembrolizumab, 10 µg/ml ipilimumab and 20 µg/ml durvalumab) and/or 400 µmol PI-9i. (*) $p < 0.05$ and (**) $p < 0.005$ in t test of sample and unstimulated control without immune modulators. Depicted are means with standard deviation of three biologically replicates.

inhibits the function of granzyme B. Indeed, at least 40 % of HROC113 as well as HROC285 T0 M2 tumor cells expressed this enzyme inhibitor (Fig. 3e). This finding seems to be common in CRC cells, since PI-9 expression was also observed in several other patient-derived CRC cell lines in varying amounts and was independent of MSI (Supplementary Fig. 4).

The analysis of secreted cytokines showed that neither HROC113 nor HROC285 T0 M2 produced IL-10 in measurable amounts, which is known to impair T cell function. Additionally, the cytokine profile of the tumor cell lines (Supplementary Fig. 5) did not explain their immunosuppressive behavior in co-culture. Fibrinogen-like protein 1 (Supplementary Fig. 6), an immunosuppressive ligand of LAG-3, was also not detectable in tumor cell culture supernatants.

T cells characterization shows exhausted and regulatory subpopulations

Poor tumor cell recognition can be caused by an impaired ability for activation due to T cell exhaustion. To assess the level of exhaustion in unspecifically expanded pTc and TiTc from patients HROC113 and HROC285, expression levels of PD-1, CTLA-4, and LAG-3 were determined. LAG-3 (pTc HROC113: 82 %; pTc HROC285: 67 %) and CTLA-4 (pTc HROC113: 68 %; pTc HROC285: 51 %) were found to be expressed on the majority of pTc, while PD-1 was present on less than 20 % of T cells (Fig. 4a, b). Exhausted T cells were classified as PD-1/CTLA-4/LAG-3 triple positive cells with 10 % of pTc HROC113 and 9 % of pTc HROC285 identified as such, respectively.

The assessment of immune checkpoint molecules on TiTc (Fig. 4c, d) revealed a larger quantity of cells positive for PD-1 in TiTc of HROC113 and HROC285 compared to the respective matching pTc ($p = 0.02$). The large proportion of PD-1$^+$ TiTc (60 % in TiTc HROC113 as well as TiTc HROC285) was accompanied by an overall enlarged population of exhausted cells in TiTc ($p = 0.05$).

Although, the amount of CD4$^+$ cells was higher in TiTc than pTc ($p < 0.001$), this did not coincide with larger amounts of regulatory T cells (Fig. 4e). In pTc HROC113, 5.2 % of the cells were CD4$^+$/CD25$^+$/FoxP3$^+$, while this population represented less than 1 % of cells among the matching TiTc ($p = 0.006$). A contrasting observation was made in pTc and TiTc HROC285, where 3.2 and 7.7 % of the cells were identified as regulatory T cells, respectively.

The cytokine detection assay in T cell and co-cultures revealed secretion of the pro-inflammatory interleukins (IL) -5, -6, and -17a as well as GM-CSF (Supplementary Fig. 5). It was frequently seen, that the cytokine concentration was highest in T cell culture and decreased in the co-culture setting, while secretion by tumor cells alone was minimal.

Peptide-stimulated T cells recognize autologous tumor cells better than co-cultured T cells

In a previous study, we showed that T cell stimulation with mutated neoantigens and non-mutated cryptic peptides improved tumor cell recognition in pTc and TiTc[20]. In the present study, we compared the strength of T cell activation mediated by these tumor-specific peptides with T cell stimulation by autologous tumor cells. pTc HROC113 and pTc HROC285 pre-stimulated with cryptic peptides reached significantly higher amounts of degranulating cells compared to all respective co-culture approaches ($p < 0.001$ in both cases) (Fig. 1a, c). A similar effect concerning improved tumor cell recognition by neoantigen stimulation was observed in pTc HROC113, but high variance prevented reaching significance. Additionally, these peptide stimulation experiments showed that tumor-specific T cell responses can be induced similarly in both pTc and TiTc, while tumor cell recognition by pTc partly even proved superior ($p_{\text{pTc HROC113 (cryptic peptides) vs TiTc HROC113 (cryptic peptides)}} = 0.01$). Furthermore, these results demonstrate, that the tumor cells are indeed immunogenic and the missing T cell response in co-culture tests must be ascribed to remarkable immunosuppressive tumor cell properties. However, since the combined ICI treatment could not improve tumor cell recognition by peptide-stimulated T cells, we assume that for these two MSI CRC cases, immunosuppression does not only depend on PD-1, PD-L1 and CTLA4.

Peptide-stimulated pTc HROC113 eliminate autologous tumor cells

Since granzyme B activity measurement was unsuitable for detecting T cell-mediated tumor cell killing, we set up an in vitro cytotoxicity assay based on crystal violet staining of adherent tumor cells. These were stimulated with IFNγ and treated with ICI and/or a PI-9i, which had been proven to successfully control tumor growth in mice by ref. 18. The effect of the PI-9i on tumor and T cell viability was tested beforehand with concentrations covering 25–1000 µM (Supplementary Fig. 7). The highest concentration not inducing cytotoxic effects, i.e., 400 µM, was chosen for application in the cytotoxicity assay.

Cytotoxicity was experimentally tested as a proof of concept with peptide-stimulated pTc HROC113, as they showed significantly better tumor cell recognition than co-cultured T cells. After 48 h of incubation with autologous tumor cells, pTc HROC113 were not able to eliminate the tumor cells and this was not significantly improved by the addition of ICI, PI-9i or the combination of both (Fig. 5). On the contrary, pTc HROC113 pre-stimulated with tumor-specific cryptic peptides or neoantigens eliminated on average 66 % ($p = 0.01$) or 78 % ($p = 0.002$) of the tumor cells, respectively. However, similarly to the findings with untreated control pTc HROC113, the addition of the above-mentioned immune modulators did not result in increased tumor cell killing. Instead, the combination of ICI and PI-9i even seemed to worsen the outcomes with all three T cell populations.

Discussion

In this study, we investigated the interaction of carefully selected tumor and autologous T cells in vitro. In initial co-culture experiments, no anti-tumor responses were observed, which was due to the clinical manifestation of the original tumors rather expected than surprising. Disappointingly, subsequent ICI treatment to re-establish T cell activity and tumor cell recognition did not work out as expected.

Resistance against ICI is either an innate tumor cell property or is observed as an acquired phenomenon after therapy. ICI resistance can be categorized into three groups: resistance mechanisms related to (I) antigen recognition; (II) T cell migration/infiltration; and (III) effector functions of

T cells[21]. When comparing gene expression of proteins involved in antigen processing[14] between our two tumor models and normal colon tissue, the majority of genes showed a higher expression in tumor than in normal tissue; hinting at a preservation of functional antigen processing. Even though B2M expression was decreased, a HLA ligandome analysis revealed thousands of HLA-eluted peptides in both cell lines[20]. Thus, the presentation of tumor-specific peptides with the potential to activate T cells was maintained in these two CRC cases, contrasting the well-established correlation of MSI and diminished HLA expression[22–24]. However, despite preserved functional tumor antigen presentation, the interaction of the T cell receptor and peptide-presenting tumor cells can be impaired, for example, by an overexpression of cell surface glycosphingolipids sterically impeding the interaction[25].

Since antigen presentation was likely not defective and the selected co-culture in vitro assay neglected the issue of T cell infiltration, the observed ICI resistance was probably caused by resistance mechanisms related to T cell effector functions. When ICI were used to interfere with PD-1 and PD-L1, which was expressed on the majority of tumor cells, there was no improvement in anti-tumor response observed, even when these ICI where combined with anti-CTLA-4. The detailed characterization of the T cell populations revealed the expression of a further immune checkpoint, namely LAG-3, on the majority of T cells, possibly impairing their activation after binding to tumor cell MHC II. Currently, several anti-LAG-3 antibodies are tested in pre-clinical and clinical trials[26]. Moreover, as TIM-3 and TIGIT also seem to negatively regulate T cell activity, blocking antibodies are similarly under investigation[27] and further immune checkpoints are identified continuously[28]. By focusing the investigations on clinically approved ICI the results of the study may be limited, but they also prove that further research is urgently needed.

The effector function of T cells is not only suppressed directly by tumor cells, but is mainly influenced by the tumor microenvironment. Here, immunosuppressive cell populations and cytokines are responsible for decreased T cell activity. The determination of regulatory T cell subsets in our selected cancer cases did not indicate strong cell-based immune inhibition as these did not exceed 10 %, which equals to regulatory T cell levels in healthy individuals[29]. Studies claiming increased proportions of regulatory T cells in peripheral blood of tumor patients compared to healthy donors[30–32] could thus not be validated in the CRC cases analyzed. Of note, T cells underwent two weeks of unspecific expansion prior to measurements, potentially changing the composition of cell subpopulations. Likely, persisting immune suppression by tumor cells in the tumor microenvironment resulted in lower anti-tumor reactivity of TiTc compared to pTc, characterized by a higher proportion of exhausted T cells or an increased state of T cell exhaustion. Moreover, secretion of known immunosuppressive cytokines like IL-10 could be excluded as driver of T cell inhibition.

Additional examinations revealed granzyme B activity in both tumor cell lines HROC113 and HROC285 T0 M2, accompanied by the expression of its inhibitor PI-9. Granzyme B, which is physiologically expressed in cytotoxic T and natural killer cells[33], was already detected previously in breast, lung, and urothelial carcinoma cells[34–36]. Moreover, the expression of PI-9, the protective shield against intracellular granzyme B activity, was found in prostate, lung, and rectal cancer[37–39] and we could confirm this finding here for a small series of low-passaged, patient-derived CRC cell lines. Since several studies showed a negative correlation between PI-9 expression and response to ICI[40,41], we hypothesized, that the use of PI-9i might restore anti-tumor immune responses.

However, the proof-of-concept cytotoxicity assay of pTc HROC113 and the tumor cell line HROC113 revealed, that neither ICI nor PI-9i treatment resulted in significant changes and even the combination failed to improve tumor cell elimination. It is thus safe to conclude, that tumor cells utilized immunosuppressive mechanisms beyond the investigated cytokine secretion, immune checkpoint expression, and adaption to cytotoxic microenvironment. Clinically, failure of ICI would have been interpreted probably as an immunological cold tumor, but T cell stimulations disproved this assumption. When T cells were stimulated with tumor-specific peptides, recognition and elimination of tumor cells increased significantly. Both, cryptic peptides as well as neoantigens, sufficiently induced T cell effector function, clearly exceeding the effects of ICI and/or PI-9i. Since our investigations included only two CRC cases, the results might not be applicable to the entirety of CRC patients, but they show the potential of immunologic modulation beyond ICI treatment.

By comparing stimulated pTc and TiTc, we further showed, that T cells from peripheral blood are a valuable source of lymphocytes, which can be turned into tumor-reactive T cells by stimulation with tumor-specific peptides. In connection with studies showing that the quality[42] and clonality[43] of neoantigens was superior in predicting T cell response in comparison to mere neoantigen number, these results hint at a likely broader applicability of immunotherapy beyond tumors with high TMB.

Nevertheless, the incomplete elimination of tumor cells by peptide-stimulated T cells might again be an indicator of a complex network of immunosuppressive mechanisms in use by the tumor cells, which must be examined further. Our data also imply, that the development of new immune modulators interfering with immunosuppressive molecules (immune checkpoint ligands, enzymes, cytokines, etc.) and tumor-individual selection of those will contribute equally to optimally support the effector function of tumor-reactive T cells. By applying ex vivo expanded and selected T cells or genetically modified CAR T cells or TCR T cells, the strength of the anti-tumor reactions might increase dramatically and could overcome immunosuppressive barriers. Additionally, the combination of strongly primed T cells with further immune modulators could prevent acquired resistance to immunotherapy and tumor relapse as several studies already showed durable responses in combination therapy[44,45].

Summarizing all results, our detailed investigation of two distinct sets of patient-derived cell populations demonstrated that ICI-resistant tumor cells can be targeted by T cells primed with tumor-specific antigens. This peptide stimulation induced increased tumor cell recognition not only in TiTc, but also in pTc, which partially even exceeded the former. These findings in pTc could hint towards an equivalent or even superior performance in future immunotherapeutic approaches. In our investigation, extensive T cell priming in a personalized approach was superior to standardized ICI therapy, underlining the importance of precision medicine also in cancer immunotherapy. Additionally, this patient-individual approach could be combined with drugs like ICI and enzyme blockers according to the respective tumor characteristics. Such multimodal approaches could then tackle the complex network of immunosuppressive strategies to successfully overcome immunological barriers erected by any given tumor.

Methods

Ethics approval and consent to participate

The study was conducted according to the guidelines of the Declaration of Helsinki. All patients gave informed written consent to participate in the study and all procedures were approved by the Ethics Committee of the University of Rostock University Medical Center (Reference numbers: A 2018-0054 and A 2019-0187) in accordance with generally accepted guidelines for the use of human material.

Cell culture

Patient-derived CRC cell lines HROC113 and HROC285 T0 M2 from the HROC collection[19] were cultured under standard conditions in DMEM/Ham´s F12 medium supplemented with 10 % FCS and 2 mM L-glutamine. For several experiments, tumor cells were treated for 48 h with 200IU/ml IFNγ (Imukin, Boehringer Ingelheim, Ingelheim am Rhein, Germany). Cell culture reagents were obtained from PAN Biotech, Aidenbach, Germany, unless stated otherwise.

T cell isolation and expansion

Isolation of peripheral blood mononuclear cells and pTc from patients´ heparinized blood as well as TiTc from vitally frozen tumor pieces was followed by a rapid Tc expansion protocol (REP) as described recently[20].

Co-culture

Co-culture was conducted by adapting a previous protocol[46]. Briefly, 20,000 IFNγ-treated tumor cells were seeded with 200,000 T cells in a 24-well plate coated with anti-human CD28 (Immunotools, Friesoythe, Germany) in DMEM/Ham´s F12 medium, 10 % human AB serum, 2 mM L-glutamine, penicillin, streptomycin and amphotericin (T cell medium) supplemented with 300 IU/ml IL-2. Every 2–3 days, half of the medium was exchanged. At day seven, cells were harvested and seeded with freshly-prepared IFNγ-treated tumor cells in a ratio of 10:1. The co-culture ended at day 14 and cells were further analyzed. The medium of several experiments was supplemented with ICI (20 µg/ml Pembrolizumab (Merck, Darmstadt, Germany); 10 µg/ml Ipilimumab (Bristol-Myers Squibb, New York City, NY, USA); or 20 µg/ml Durvalumab (AstraZeneca, Cambridge, UK)).

T cell stimulation

Autologous B lymphoid cell lines (B-LCL) were used as antigen presenting cells. For peptide-loading, 3×10^6 B-LCLs were incubated at 37 °C with 10 µg peptide pools in 1 ml serum free medium for 1 h. Stimulations were performed in 24-well plates with irradiated (30 Gy) peptide-loaded B-LCL added at a ratio of 1:4 to 1×10^6 expanded T cells in 2 ml of T cell medium supplemented with 1xITS solution IV and 300 IU/ml IL-2 per well. After seven days of co-culture, T cells were harvested, counted, and re-stimulated. T cells stimulated with B-LCLs without any peptide served as controls.

Flow cytometry

Tumor and T cells were collected and washed with phosphate-buffered saline (PBS). For extracellular staining, cells were incubated in 100 µl staining buffer (PBS, 200 mM EDTA, 0.5 % bovine serum albumin) with the appropriate volume of antibody for 30 min at 4 °C protected from light. After centrifugation, the staining solution was discarded and cells were washed again with staining buffer. Stained cells were resuspended in staining buffer and measured promptly. Intracellular staining was performed using the InsideStain Kit (Miltenyi Biotec) according to the manufacturer's instructions and measured promptly. The following anti-human antibodies were used from Immunotools CD4-APC, CD8-APC, CD25-FITC, and FoxP3-PE or Biolegend (San Diego, CA, USA): CD107a-FITC, CD152-PE, CD223-APC, CD274-FITC, and CD279-FITC. Samples were measured using a BD FACSCalibur™ and data was analyzed by using FCSalyzer 0.9.21 alpha (Sven Mostböck, Vienna, Austria; https://sourceforge.net/projects/fcsalyzer/).

Degranulation assay

The ability of T cells to recognize tumor cells was tested in the degranulation assay[46]. A 96-well plate was coated with anti-human CD28 (Immunotools) and 100,000 IFNγ-treated tumor cells were seeded together with 200,000 pTc or TiTc per well in Tc medium containing anti-human CD107a-FITC (Biolegend). After 1 h incubation, 1 µg/ml Brefeldin A (MedChemExpress, Monmouth Junction, NJ, USA) was added, followed by another 4 h incubation. Intracellular flow cytometry staining was conducted as described using CD8-APC (Immunotools) and IFNγ-PE (Biolegend). Samples were measured with gates adjusted to detect $CD8^+/CD107a^+/IFN\gamma^+$ cells. To receive values for relative degranulation, percentage of triple-positive T cells was normalized to the triple-positive population in T cells not incubated with tumor cells.

Cytokine detection and FGL1 ELISA

For cytokine detection, supernatants were collected from T cells, tumor cells and co-cultures, all cultured for seven days without medium exchange. The concentrations of granulocyte-macrophage colony-stimulating factor (GM-CSF), IFNα, IFNγ, lL-2, IL-4, IL-5, IL-6, IL-9, IL-10, IL-12p70, IL-17A, and tumor necrosis factor were determined by MACSPlex Cytokine 12 Kit (Miltenyi Biotec). Supernatants of tumor cell lines were also used for the measurement of FGL-1 with the Human FGL1/Fibrinogen Like Protein 1 ELISA Kit (Assay Genie, Dublin, Ireland).

GranToxiLux

The GranToxiLux assay was performed according to manufacturer's instructions (Oncoimmunin Inc, Gaithersburg, MD, USA).

Cytotoxicity assay

Tumor cells were seeded into a 48 well plate and stimulated with 200 IU/ml IFNγ for 48 h. Simultaneously, respective wells were treated with 400 µM PI-9i (1,3-Benzoxazole-6-carboxylic acid, Advanced ChemBlocks Inc, Hayward, CA, USA). Following pre-treatment, 5×10^5 peptide-stimulated or control Tc were added to the approximately 1×10^5 tumor cells in each well. The number of tumor cells was estimated using previously determined doubling times. The co-culture medium was supplemented with ICI (20 µg/ml Pembrolizumab; 10 µg/ml Ipilimumab; 20 µg/ml Durvalumab) and/or PI-9i (400 µM). After 48 h of co-culture, medium was discarded, wells were washed once with PBS before 200 µl of 0.2 % crystal violet solution was added. After 20 min incubation at room temperature, staining solution was discarded and wells were washed three times with PBS. When plates were dry, 500 µl of sodium dodecyl sulfate solution was added and optical density at 570 nm was measured at the microplate reader Infinite 200 (Tecan, Männedorf, Switzerland).

RNA expression analysis

RNA sequencing of the patient-derived cell lines was performed by the Center for Quantitative Biology (QBiC, University of Tübingen, Germany) and resulting data was provided. RNA from cell pellets was isolated using the QIAsymphony RNA kit on the QIAsymphony SP platform (Qiagen, Venlo, Netherlands). Upon the completion of the protocol, the RNA was eluted in 80 µl of RNase-free water. The concentration of RNA was measured using the Qubit Fluorometric Quantitation and RNA Broad-Range Assay (Thermo Fisher Scientific, Waltham, MA, USA). RNA Integrity Number RIN was determined using the Fragment Analyzer 5300 and the Fragment Analyzer RNA kit (Agilent Technologies, Santa Clara, CA, USA) and presented a good integrity (RIN >9). For library preparation, the mRNA fraction was enriched using polyA capture from 200 ng of total RNA using the NEBNext Poly(A) mRNA Magnetic Isolation Module (New England Biolabs, Ipswich, MA, USA). Subsequently, libraries were prepared using the NEB Next Ultra II Directional RNA Library Prep Kit for Illumina and NEBNext UDI (New England Biolabs) following the manufacturer's instructions. To minimize technical batch effects, library preparations were performed using the liquid handler Biomek i7 (Beckman Coulter, Brea, CA, USA). The library molarity was determined by measuring the library size (approximately 390 bp) using the Fragment Analyzer 5300 and the Fragment Analyzer DNA HS NGS fragment kit (Agilent Technologies) and the library concentration (>1 ng/µl) using Qubit Fluorometric Quantitation and dsDNA High sensitivity assay (Thermo Fisher Scientific). The libraries were denaturated according to the manufacturer's instructions, diluted to 265 pM and sequenced as paired-end 100 bp reads on an Illumina NovaSeq 6000 (Illumina, San Diego, CA, USA). The sequencing aimed to achieve a depth of approximately 26 million clusters in mean per sample.

Read quality of RNA-seq data in fastq files was assessed using ngs-bits, to identify sequencing cycles with low average quality, adaptor contamination, or repetitive sequences from PCR amplification. Reads were aligned using STAR[47] to the GRCh38 and alignment quality was analyzed using ngs-bits and visually inspected in the Integrative Genome Viewer. Normalized read counts for all genes were obtained using Subread and edgeR.

Raw gene expression was filtered by demanding a minimum expression value of 1 cpm (counts per million) in at least 2 samples. The distribution of logarithmized cpm-normalized expression values shows similar characteristics over all samples. Based on the filtered data set, samples were investigated with respect to their pairwise similarity. Spearman's rank correlation coefficient was calculated for each pair of samples. A hierarchical clustering was performed on the resulting similarity values. Differential gene expression analysis was conducted based on the filtered gene expression data set. A statistical model incorporating the group property of samples was

tested by fitting a negative binomial distribution using a generalized linear model approach. For each gene, gene expression fold changes (log2 fold change) were computed and a statistical test was performed to assess the significance, which is given as raw *p* value and adjusted *p* value (FDR).

Moreover, publicly available data was used for comparison. First, R package (R (4.2.1) version) was applied to The Cancer Genome Atlas (TCGA, https://portal.gdc.cancer.gov/ (accessed on 20.06.2022)) and the Genotype-Tissue Expression (GTEx, gtexportal.org/home/ (accessed on 20.06.2022)) databases to analyze the difference of the mRNA levels of 18 genes of interest including ERAP1 [ENSG00000164307.12], ERAP2 [ENSG00000164308.16], PDIA3 [ENSG00000167004.12], PSMB5 [ENSG00000100804.18], PSMB6 [ENSG0000142507.9], PSMB7 [ENSG00000136930.12], PSMB8 [ENSG00000204264.8], PSMB9 [ENSSG00000240065.7], PSMB10 [ENSG00000205220.11], B2M [ENSG00000166710.17], CALR [ENSG00000179218.13], CANX [ENSG00000127022.14], TAP1 [ENSG00000168394.10], TAP2 [ENSG00000204267.13], TAPBP [ENSSG00000231925.11], HLA-A [ENSG00000206503.11], HLA-B [ENSG00000234745.9] and HLA-C [ENSG00000204525.14]. Gene expression was compared between 484 CRC and 359 normal colorectal mucosal tissue samples. Moreover, TMB was used to group the cancer samples: Samples were sorted by TMB and top 20 % were identified as TMB high. Remaining samples were considered TMB low.

Statistical analyses

Statistical significance was determined by an unpaired, two-sided *t* test using GraphPad Prism 5 (Boston, MA, USA). Results were stated significant if the *t* test resulted in $p < 0.05$. Details on compared groups are given in the figure legends. If not stated otherwise, graphs depicting the results show mean values and the respective standard deviation of distinct samples.

Data availability

RNA Sequencing data obtained in the study are available in a public, open access repository (NCBI BioSample: SAMN41078298). The biomaterials analyzed in the current study are available from the corresponding author on reasonable request.

Received: 23 January 2024; Accepted: 9 July 2024;
Published online: 29 July 2024

References

1. Campoli, M. & Ferrone, S. HLA antigen changes in malignant cells: epigenetic mechanisms and biologic significance. *Oncogene* **27**, 5869–5885 (2008).
2. Moon, J., Oh, Y. M. & Ha, S.-J. Perspectives on immune checkpoint ligands: expression, regulation, and clinical implications. *BMB Rep.* **54**, 403–412 (2021).
3. Klempner, S. J. et al. Tumor mutational burden as a predictive biomarker for response to immune checkpoint inhibitors: a review of current evidence. *Oncologist* **25**, e147–e159 (2020).
4. Le, D. T. et al. PD-1 blockade in tumors with mismatch-repair deficiency. *N. Engl. J. Med.* **372**, 2509–2520 (2015).
5. Overman, M. J. et al. Nivolumab in patients with metastatic DNA mismatch repair-deficient or microsatellite instability-high colorectal cancer (CheckMate 142): an open-label, multicentre, phase 2 study. *Lancet Oncol.* **18**, 1182–1191 (2017).
6. Oh, C. R. et al. Phase II study of durvalumab monotherapy in patients with previously treated microsatellite instability-high/mismatch repair-deficient or POLE-mutated metastatic or unresectable colorectal cancer. *Int. J. cancer* **150**, 2038–2045 (2022).
7. Overman, M. J. et al. Durable clinical benefit with Nivolumab Plus Ipilimumab in DNA mismatch repair-deficient/microsatellite instability-high metastatic colorectal cancer. *J. Clin. Oncol.* **36**, 773–779 (2018).
8. Ganesh, K. et al. Immunotherapy in colorectal cancer: rationale, challenges and potential. *Nat. Rev. Gastroenterol. Hepatol.* **16**, 361–375 (2019).
9. Aptsiauri, N. & Garrido, F. The challenges of HLA Class I loss in cancer immunotherapy: facts and hopes. *Clin. Cancer Res.* **28**, 5021–5029 (2022).
10. Li, Y. et al. Tumor mutational burden predicting the efficacy of immune checkpoint inhibitors in colorectal cancer: a systematic review and meta-analysis. *Front. Immunol.* **12**, 751407 (2021).
11. Strickler, J. H., Hanks, B. A. & Khasraw, M. Tumor mutational burden as a predictor of immunotherapy response: is more always better? *Clin. Cancer Res.* **27**, 1236–1241 (2021).
12. Zhang, X. et al. Integrated investigation of the prognostic role of HLA LOH in advanced lung cancer patients with immunotherapy. *Front. Genet.* **13**, 1066636 (2022).
13. Shim, J. H. et al. HLA-corrected tumor mutation burden and homologous recombination deficiency for the prediction of response to PD-(L)1 blockade in advanced non-small-cell lung cancer patients. *Ann. Oncol.* **31**, 902–911 (2020).
14. Wang, S., He, Z., Wang, X., Li, H. & Liu, X.-S. Antigen presentation and tumor immunogenicity in cancer immunotherapy response prediction. *eLife* **8**; https://doi.org/10.7554/eLife.49020 (2019).
15. Kim, R., Emi, M., Tanabe, K. & Arihiro, K. Tumor-driven evolution of immunosuppressive networks during malignant progression. *Cancer Res.* **66**, 5527–5536 (2006).
16. Burkholder, B. et al. Tumor-induced perturbations of cytokines and immune cell networks. *Biochim. et. Biophys. Acta* **1845**, 182–201 (2014).
17. Zhai, L. et al. Immunosuppressive IDO in cancer: mechanisms of action, animal models, and targeting strategies. *Front. Immunol.* **11**, 1185 (2020).
18. Jiang, L. et al. Direct tumor killing and immunotherapy through Anti-SerpinB9 therapy. *Cell* **183**, 1219–1233.e18 (2020).
19. Mullins, C. S. et al. Integrated biobanking and tumor model establishment of human colorectal carcinoma provides excellent tools for preclinical research. *Cancers* **11**; https://doi.org/10.3390/cancers11101520 (2019).
20. Schwarz, S. et al. T cells of colorectal cancer patients' stimulated by neoantigenic and cryptic peptides better recognize autologous tumor cells. *J. Immunothe. Cancer* **10**; https://doi.org/10.1136/jitc-2022-005651 (2022).
21. Nagasaki, J., Ishino, T. & Togashi, Y. Mechanisms of resistance to immune checkpoint inhibitors. *Cancer Sci.* **113**, 3303–3312 (2022).
22. Bicknell, D. C., Kaklamanis, L., Hampson, R., Bodmer, W. F. & Karran, P. Selection for beta 2-microglobulin mutation in mismatch repair-defective colorectal carcinomas. *Curr. Biol.* **6**, 1695–1697 (1996).
23. Kloor, M. et al. Immunoselective pressure and human leukocyte antigen class I antigen machinery defects in microsatellite unstable colorectal cancers. *Cancer Res.* **65**, 6418–6424 (2005).
24. Kloor, M. et al. Beta2-microglobulin mutations in microsatellite unstable colorectal tumors. *Int. J. cancer* **121**, 454–458 (2007).
25. Jongsma, M. L. M. et al. The SPPL3-defined glycosphingolipid repertoire Orchestrates HLA Class I-mediated immune responses. *Immunity* **54**, 132–150.e9 (2021).
26. Sauer, N. et al. LAG-3 as a potent target for novel anticancer therapies of a wide range of tumors. *Int. J. Mol. Sci.* **23**; https://doi.org/10.3390/ijms23179958 (2022).
27. Cai, L., Li, Y., Tan, J., Xu, L. & Li, Y. Targeting LAG-3, TIM-3, and TIGIT for cancer immunotherapy. *J. Hematol. Oncol.* **16**, 101 (2023).
28. Wang, Y. et al. Immune checkpoint modulators in cancer immunotherapy: recent advances and emerging concepts. *J. Hematol. Oncol.* **15**, 111 (2022).
29. Taams, L. S. et al. Regulatory T cells in human disease and their potential for therapeutic manipulation. *Immunology* **118**, 1–9 (2006).
30. Liyanage, U. K. et al. Prevalence of regulatory T cells is increased in peripheral blood and tumor microenvironment of patients with pancreas or breast adenocarcinoma. *J. Immunol.* **169**, 2756–2761 (2002).

31. Ormandy, L. A. et al. Increased populations of regulatory T cells in peripheral blood of patients with hepatocellular carcinoma. *Cancer Res.* **65**, 2457–2464 (2005).
32. Wolf, A. M. et al. Increase of regulatory T cells in the peripheral blood of cancer patients. *Clin. Cancer Res.* **9**, 606–612 (2003).
33. Cullen, S. P., Brunet, M. & Martin, S. J. Granzymes in cancer and immunity. *Cell Death Differ.* **17**, 616–623 (2010).
34. D'Eliseo, D. et al. Granzyme B is expressed in urothelial carcinoma and promotes cancer cell invasion. *Int. J. Cancer* **127**, 1283–1294 (2010).
35. Hu, S. X. et al. Expression of endogenous granzyme B in a subset of human primary breast carcinomas. *Br. J. Cancer* **89**, 135–139 (2003).
36. Kontani, K. et al. Involvement of granzyme B and perforin in suppressing nodal metastasis of cancer cells in breast and lung cancers. *Eur. J. Surg. Oncol.* **27**, 180–186 (2001).
37. Ray, M., Hostetter, D. R., Loeb, C. R. K., Simko, J. & Craik, C. S. Inhibition of Granzyme B by PI-9 protects prostate cancer cells from apoptosis. *Prostate* **72**, 846–855 (2012).
38. Repetto, O. et al. Identification of protein clusters predictive of tumor response in rectal cancer patients receiving neoadjuvant chemo-radiotherapy. *Oncotarget* **8**, 28328–28341 (2017).
39. Soriano, C. et al. Increased proteinase inhibitor-9 (PI-9) and reduced granzyme B in lung cancer: mechanism for immune evasion? *Lung Cancer* **77**, 38–45 (2012).
40. Jiang, P. et al. Signatures of T cell dysfunction and exclusion predict cancer immunotherapy response. *Nat. Med.* **24**, 1550–1558 (2018).
41. Ibáñez-Molero, S. et al. SERPINB9 is commonly amplified and high expression in cancer cells correlates with poor immune checkpoint blockade response. *Oncoimmunology* **11**, 2139074 (2022).
42. Balachandran, V. P. et al. Identification of unique neoantigen qualities in long-term survivors of pancreatic cancer. *Nature* **551**, 512–516 (2017).
43. McGranahan, N. et al. Clonal neoantigens elicit T cell immunoreactivity and sensitivity to immune checkpoint blockade. *Science* **351**, 1463–1469 (2016).
44. Wilgenhof, S. et al. Phase II study of autologous monocyte-derived mRNA electroporated dendritic cells (TriMixDC-MEL) Plus Ipilimumab in patients with pretreated advanced melanoma. *J. Clin. Oncol.* **34**, 1330–1338 (2016).
45. Zhao, J., Chen, Y., Ding, Z.-Y. & Liu, J.-Y. Safety and efficacy of therapeutic cancer vaccines alone or in combination with immune checkpoint inhibitors in cancer treatment. *Front. Pharmacol.* **10**, 1184 (2019).
46. Cattaneo, C. M. et al. Tumor organoid-T-cell coculture systems. *Nat. Protoc.* **15**, 15–39 (2020).
47. Dobin, A. et al. STAR: ultrafast universal RNA-seq aligner. *Bioinformatics* **29**, 15–21 (2013).

Acknowledgements

The authors express their gratitude to the patients for participating in the HROC collection. This research was in part funded by grant number TBI-V-1-241-VBW-084 and TBI-V-240-VBW-084 from the state Mecklenburg-Vorpommern.

Author contributions

Design and conceptualization of the study was directed by M.L. Experimental design, data interpretation and formal analysis was performed by S.S. M.K. established the patient-derived cell lines and S.Z. analyzed expression data. Identification and validation of cryptic peptides and neoantigens was performed by M.W.L. and A.S. The initial draft and figures were prepared by S.S. and M.L.; S.Z., M.K., M.W.L., and A.S. reviewed and edited the manuscript. All authors have read and agreed to the final version of the manuscript.

Funding

Open Access funding enabled and organized by Projekt DEAL.

Competing interests

M.W.L. is an inventor of patents owned by Immatics Biotechnologies and has acted as a speaker and paid consultant in cancer immunology for Boehringer Ingelheim. The other authors do not declare conflicting interests.

Additional information

Supplementary information The online version contains supplementary material available at https://doi.org/10.1038/s41698-024-00645-3.

Correspondence and requests for materials should be addressed to Michael Linnebacher.